

Heterogeneous Graph Neural Network with Multi-view Representation Learning

Zezhi Shao, Yongjun Xu, Wei Wei, Fei Wang, Zhao Zhang, Feida Zhu

Abstract—Graph neural networks for heterogeneous graph embedding is to project nodes into a low-dimensional space by exploring the heterogeneity and semantics of the heterogeneous graph. However, on the one hand, most of existing heterogeneous graph embedding methods either insufficiently model the local structure under specific semantic, or neglect the heterogeneity when aggregating information from it. On the other hand, representations from multiple semantics are not comprehensively integrated to obtain versatile node embeddings. To address the problem, we propose a *Heterogeneous Graph Neural Network with Multi-View Representation Learning* (named MV-HetGNN) for heterogeneous graph embedding by introducing the idea of multi-view representation learning. The proposed model consists of node feature transformation, view-specific ego graph encoding and auto multi-view fusion to thoroughly learn complex structural and semantic information for generating comprehensive node representations. Extensive experiments on three real-world heterogeneous graph datasets show that the proposed MV-HetGNN model consistently outperforms all the state-of-the-art GNN baselines in various downstream tasks, *e.g.*, node classification, node clustering, and link prediction.

Index Terms—Heterogeneous graphs, graph neural networks, Graph embedding.

1 INTRODUCTION

GRAPH structured data is ubiquitous in the real world, such as social networks [1], [2], [3], [4] and citation networks [5], [6]. In recent years, *graph neural networks* (GNNs) have become one of the standard paradigms for analyzing graph structured data. The core idea of GNNs is to explore the multi-hop local structure of the target node, *i.e.*, the *ego network* or *ego graph* [7], by stacking multiple layers. As a basic graph structure, homogeneous graphs consist of only one type of nodes and edges, and the ego graph in it has a clear definition and intuition [8], *e.g.*, *first-order* or *second-order* structure. Therefore, GNNs have achieved great success on homogeneous graphs. [5], [6].

However, traditional GNN-based approaches cannot be directly applicable to *heterogeneous graphs* (HGs) because they ignore two basic properties of HGs, *i.e.*, the **heterogeneity** and **semantics**. An example of an ego graph depicting the complex local structure in HGs is shown in Figure 1(a). *Firstly*, the ego graph of HGs is equipped with many types of nodes and relations, *i.e.*, **heterogeneity**. The features of different types of nodes fall in different feature spaces, hindering the aggregation operation of GNNs. For example, the *Author* nodes need to be projected into the feature space of the *Paper* nodes through the *Write* relation so as to aggregate with other *Paper* nodes. *Second*, many

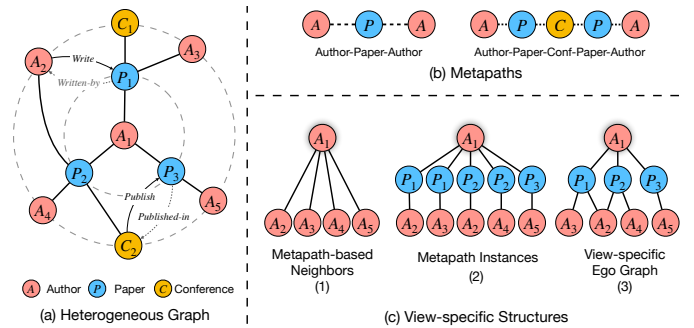


Fig. 1. An illustrative example of heterogeneous graph (DBLP) and some key concept. (a) A heterogeneous graph DBLP. (b) Two metapaths for DBLP. (c) Three types of metapath-based local structures of author node 0 (based on metapath *APA*) proposed by HAN [9], MAGNN [10], and our EGGNN.

meaningful and complex semantic information implicitly exists in the ego graph of HGs, *i.e.*, **semantics**. These implicit but important relationships are captured by high-order relations, *i.e.*, *metapath*. Different metapaths reveal different semantics, which can be regarded as a view to observe the target node's local structure. For example, as shown in Figure 1(b), *Author-Paper-Author* (APA) indicates the co-author relationship while the *A-P-Conference-P-A* indicates the co-conference relationship. These multiple view information need to be comprehensively encoded to get a versatile node embedding.

In order to apply GNNs on HGs, a number of works have emerged recently. Given the two properties mentioned above, we divide them into two categories. The first category focuses on heterogeneity. They model type-specific mapping functions to project heterogeneous nodes to the same feature space to eliminate heterogeneity when applying GNNs. However, these methods do not make efficient use of semantics [11], [12], [13],

Zezhi Shao, Yongjun Xu, Fei Wang and Zhao Zhang are with the Institute of Computing Technology, CAS, Beijing 100190, China. Zezhi Shao is also with the University of Chinese Academy of Sciences, Beijing 100049, China. (e-mail: shaozezhi19b@ict.ac.cn; xjy@ict.ac.cn; wangfei@ict.ac.cn; zhangzhao2021@ict.ac.cn)

Wei Wei is with the School of Computer Science and Engineering, Huazhong University of Science and Technology, Hubei 430074, China (e-mail: weiw@hust.edu.cn).

Feida Zhu is with the School of Information Systems, Singapore Management University, 178902 Singapore (e-mail: fdzhu@smu.edu.sg).

Corresponding Author: Wei Wei, weiw@hust.edu.cn and Fei Wang, wangfei@ict.ac.cn.

Manuscript received xxx xx, 2021; revised xxx xx, 2021.

[14], [15], [16]. Simply stacking multiple layers to catch high-order information will cause lower-order semantic information to face the over-smooth problem due to the different lengths of semantics in HGs. Instead, the second category explicitly utilizes metapath as semantics to guide information diffusion. However, they still suffer from at least one of the following limitations. (1) The methods insufficiently model the local structures based on metapath. For example, HAN [9] discard the intermediate nodes; MAGNN [10] aggregates information at *metapath instance* level, *i.e.*, the sequence level, and neglects the overall graph structure of the local structure, which cause information loss in the aggregation process. Our ablation experiments on it also demonstrated it. (2) The methods neglect to model the mapping functions between different types of nodes [17], [18] when encoding the metapath-based local structures. Some works only project them to the same dimension [9], [19], [20] and aggregate heterogeneous features directly, ignoring the mapping relation between heterogeneous nodes. (3) The interaction characteristics between multiple semantic information are not fully utilized. Most methods use the attention mechanism to softly *select* most meaningful metapaths [9], [10], [19] rather than fuse them comprehensively. They can not theoretically guarantee versatile node embeddings, *i.e.*, superior to single view representation.

To tackle these problems, we introduce the idea of multi-view learning to heterogeneous graph embedding, HG embedding is modeled as a *Multi-view Representation Learning* (MvRL) problem. MvRL aims to comprehensively encode information from multiple views into a latent representation, which is versatile with theoretical guarantee compared to any single view [21], [22]. The intuitive idea of introducing MvRL is that the semantics property of HGs matches with the idea of MvRL, *i.e.*, each view (semantics) can be regarded as a perspective to observe the target node's local structure. Therefore, the original complete ego graph in HGs can be decomposed to a set of view-specific ego graphs (or metapath-based ego graphs). Based on the idea of MvRL, we propose a *Heterogeneous Graph Neural Network based on Multi-view Representation Learning* (MV-HetGNN) for HG embedding. MV-HetGNN addresses all the issues mentioned above by three components: node feature transformation, view-specific ego graph encoding, and auto multi-view fusion. Specifically, MV-HetGNN first applies type-specific transformations to unify feature dimensions. Then, MV-HetGNN conducts view-specific ego graph encoding for every view-specific ego graph, which sufficiently models the local structure under each semantics. During this component, the representations of relations are learned to model the mapping function between heterogeneous nodes to address the heterogeneity. Finally, the auto multi-view fusion comprehensively integrates the embeddings from different views to obtain more versatile node embeddings using hierarchical autoencoder.

In general, our method extends the second category by solving many problems. Note that ordinary multi-view graph learning refers to learning on a kind of special HG that contains only one type of node and multiple types of relations. Moreover, MV-HetGNN is obviously different from methods such as HGT [16] that stacks multiple layers. In MV-HetGNN, information passing is guided by the view-specific ego graph, which can effectively alleviate over-smoothing and utilize semantic information. In summary, this work makes several major contributions:

- We propose a novel view-specific ego graph encoding module which sufficiently model and encode the local structure of the target node under specific semantics.

- We propose a novel auto multi-view fusion module, which comprehensively integrates the embeddings from different views to obtain more versatile node embeddings with theoretical guarantee. Moreover, we design orthogonal regularization for it.
- We conduct extensive experiments on three public real-world HG datasets with three different tasks. The experimental results demonstrate the superiority of MV-HetGNN over seven state-of-the-art models.

2 RELATED WORK

2.1 Graph Neural Networks

Graph Neural Networks (GNNs) are proposed to apply deep neural networks to deal with graph-structured data. GNNs can be divided into two categories: spectral-based and spatial-based methods. Spectral-based GNNs define convolution operations in the Fourier domain by computing the eigendecomposition of graph Laplacian [6], [23], [24]. Therefore, these models usually require an entire graph as input, and the eigendecomposition is computationally expensive, making them inefficient and lacking generalization ability.

Spatial-based GNNs [5], [25] define convolution operations directly in the graph domain by aggregating the information from the target nodes' local structures [26], *i.e.*, ego graph [7]. For example, GAT [25] aggregates information according to the importance score of neighborhoods assigned by a masked self-attention layer [27]. Recently, many new powerful GNN models and theories [28], [29], [30] have been proposed, which improve the representation power of GNNs. In order to exceed the expressive power of the 1-WL test, ID-GNN [7] assigns different message-passing parameters to the central node and other nodes when aggregating information from the ego graph. Due to their high efficiency, strong performance, and generalization ability, spatial GNNs have become mainstream. However, these powerful models and theories are built for homogeneous graphs, in which the local structure is well defined and has good intuition, *e.g.*, first-order, second-order [8]. The unique properties of HGs, **heterogeneity** and **semantics**, are not considered. Hence, they cannot be directly adapted to HGs.

2.2 Heterogeneous Graph Neural Networks

Heterogeneous GNN models [9], [10], [11], [12], [13], [16], [19], [31], [32], [33], [34], [35] extend GNN techniques on HGs to fully use the rich node features and semantic information. According to the two basic properties of HGs, GNNs can be divided into two categories.

The first category focuses on modelling the heterogeneity of the ego graph. These models eliminate heterogeneity by modelling mapping functions to project heterogeneous nodes to the same feature space to apply GNNs. For example, HGT [16] introduces the node- and edge-type dependent attention mechanism to handle graph heterogeneity. HetSANN [12] uses edge-type specific transformation operations to project the hidden state in the space of source node type to the hidden space of the target node type. CompGCN [14] uses composition operations, such as TransE [36] or DistMult [37], to model the mapping function efficiently by learning edge representation vectors. Although they try to thoroughly model the heterogeneity to apply GNNs, the semantics property of HGs are not fully utilized. Since the order

of semantic information is inconsistent, *e.g.*, *APA* and *APCPA* in DBLP dataset, simply stacking multiple layers to catch high-order semantic information will cause lower-order semantic information to face the over-smooth problem.

The second category focuses on semantics. These models explicitly utilize semantic information (captured by meta-paths) to analyze the ego graph. These models explicitly utilize semantic information (captured by meta-paths) to analyze the ego graph. Specifically, these methods are generally divided into two steps. *First*, the ego graph is decomposed by multiple metapaths to get local structures, which are further encoded to get node representations under each semantics. For example, as shown in Figure 1(c) HAN [9] and HGSRec [20] model the local structure under each semantics as metapath-based neighbours. However, they discard all intermediate nodes along metapath. MAGNN [10] fixes that by aggregating information at the metapath instance level, *i.e.*, sequence level. However, the graph structure of local structures is neglected, which causes information loss in the aggregation process. Similar to our model, several works leverage graph-like structures to model the local structure under each semantics, such as MEIRec [17], RecoGCN [18], T-GCN [19]. However, MEIRec neglects the feature information of intermediate and target nodes. In addition, they all ignore the modelling of mapping functions between heterogeneous nodes. *Second*, diverse semantics need to be exploited to get superior representations. Attention-based methods are widely used in these models [9], [10], [18], [19], [20] to softly select the most meaningful metapath and fuse the representations under different semantics. However, the interactive characteristics between multiple semantic information have not been fully utilized and the final representations cannot be guaranteed theoretically superior to any single semantic representation.

In general, although the heterogeneous graph neural networks have made notable progress, these problems still hinders the performance of heterogeneous graph neural networks, and there is still much room for improvement by solving these problems.

3 PROBLEM DEFINITION

Definition 1. Heterogeneous Graph. A heterogeneous graph $\mathcal{G} = (\mathcal{V}, \mathcal{E}; \phi, \omega)$ is composed of a vertex set \mathcal{V} and an edge set \mathcal{E} , along with object type mapping function $\phi : \mathcal{V} \rightarrow \mathcal{A}$ and edge type mapping function $\omega : \mathcal{E} \rightarrow \mathcal{R}$. \mathcal{A} and \mathcal{R} denote the predefined sets of object types and edge types, respectively, where $|\mathcal{A}| + |\mathcal{R}| > 2$. \mathcal{R} could be further split into two subsets: \mathcal{R}^+ and \mathcal{R}^- . Note that *self loop* relation can be randomly included in one of the two categories. An example is given in Figure 1(a).

Definition 2. Metapath. Consider $A_i \in \mathcal{A}$ and $R_i \in \mathcal{R}$ denote a node type and an edge type, respectively, a metapath P is defined as a path in the form of $A_1 \xrightarrow{R_1} A_2 \xrightarrow{R_2} \dots \xrightarrow{R_l} A_{l+1}$, which describes a composite relation $R = R_1 \circ R_2 \circ \dots \circ R_l$ between object types A_1 and A_{l+1} , where \circ denotes the composition operator over relations. Examples are given in Figure 1(b).

Definition 3. Metapath based Ego Graph. Given a metapath $P : A_1 \rightarrow A_2 \rightarrow \dots \rightarrow A_N$ and a target node v with type A_N , the ego graph (\mathcal{EG}_v^P) is a directed graph induced by the metapath-based neighborhoods and intermediate nodes along metapaths as well as v itself. An example is shown in Figure 1(c).

TABLE 1
Important notations used in this paper.

Notations	Definitions
\mathcal{V}	The set of nodes in a graph
\mathcal{A}	The set of node types
\mathcal{E}	The set of edges in a graph
\mathcal{R}	The set of edge types, <i>i.e.</i> , relations
\mathcal{G}	A graph $\mathcal{G} = \{\mathcal{V}, \mathcal{E}\}$
P	A metapath
\mathcal{P}	The set of metapaths
v	A node $v \in \mathcal{V}$
r	A kind of relation $r \in \mathcal{R}$
\mathcal{N}_v	The set of neighbors of node v
\mathcal{EG}_v^P	The ego graph of node v under metapath P
\mathbf{h}_v	Hidden state of node v
\mathbf{h}_r	Hidden state of relation r
\mathbf{H}	Hidden states of nodes with the same node type
\odot	The hadamard product
$ \cdot $	The cardinality of a set
$\ \cdot\ _F$	Frobenius norm of a matrix
$\ \cdot\ _1$	L1 norm of a matrix

Definition 4. Heterogeneous Graph Embedding. Heterogeneous graph embedding aims to learn a function that embeds the nodes in $\mathcal{G} = (\mathcal{V}, \mathcal{E}; \phi, \omega)$ into a d -dimensional Euclidean space where $d \ll |\mathcal{V}|$.

Definition 5. Versatility of Multi-View Representations. [21]

Given representations $\mathbf{h}^1, \dots, \mathbf{h}^V$ from V views, the multi-view representation \mathbf{h} is of versatility if $\forall v$ and \forall mapping $\varphi(\cdot)$ with $y^v = \varphi(\mathbf{h}^v)$, there exists a mapping $\psi(\cdot)$ satisfying $y^v = \psi(\mathbf{h})$.

4 THE PROPOSED FRAMEWORK

In this section, we present the MV-HetGNN. Our model follows the idea of multi-view representation learning and treats semantics (captured the metapaths) as a view of observing nodes. As shown in Figure 2, MV-HetGNN contains three primary steps. First, since different node types are associated with features of the different number of dimensions, the node feature transformation converts them into features of the same dimension. Then, we treat each semantic P as the view to observe target nodes' local structure and conduct view-specific ego graph encoding to sufficiently obtain the node embeddings under each view. Finally, the auto multi-view fusion module comprehensively integrates the embeddings from different views to obtain more versatile node embeddings.

4.1 Node Feature Transformation

Feature vectors of different dimensions are troublesome when aggregating information in subsequent modules. To address this issue, we apply node-type specific transformations to convert heterogeneous feature vectors into features of the same dimension. Given any node type $A_i \in \mathcal{A}$, the node feature transformation layer can be shown as follows:

$$\mathbf{H}'_{A_i} = \sigma(\mathbf{X}_{A_i} \mathbf{W}_{A_i}), \quad (1)$$

where $\mathbf{H}'_{A_i} \in \mathbb{R}^{|\mathcal{V}_{A_i}| \times d'}$ is the transformed latent vectors of nodes of A_i type. $\mathbf{X}_{A_i} \in \mathbb{R}^{|\mathcal{V}_{A_i}| \times d_{A_i}}$ is the original feature vector of all A_i nodes. $\mathbf{W}_{A_i} \in \mathbb{R}^{d_{A_i} \times d'}$ is the type-specific parameters, and

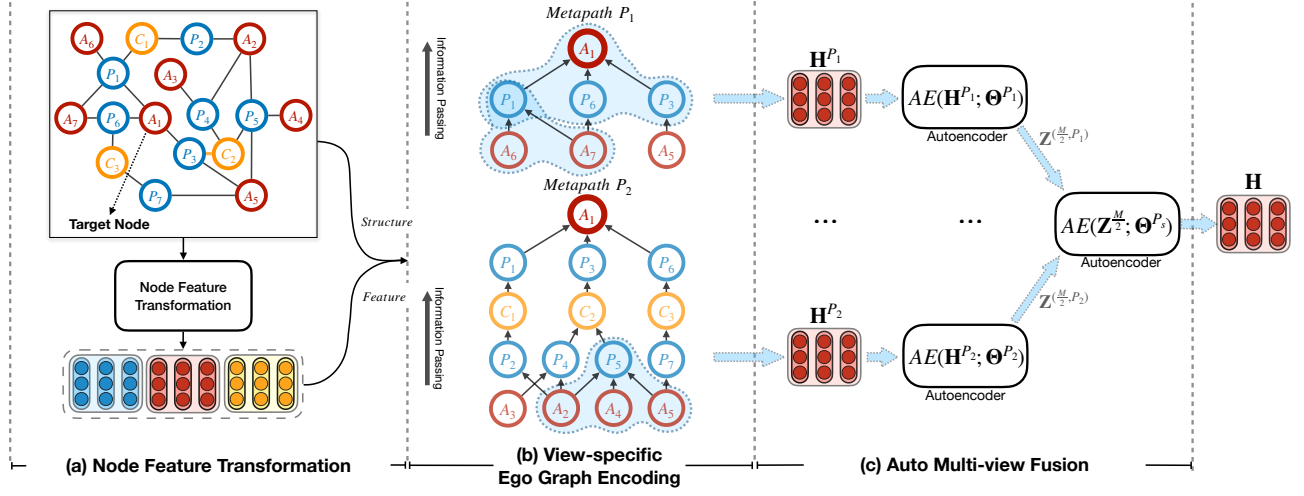


Fig. 2. The overall architecture of MV-HetGNN. (a) Node feature transformation projects the feature vectors of all types of nodes to the same dimension. (b) View-specific ego graph encoding generates embedding for a target node under each view, such as A_1 in the picture above. (c) Auto multi-view fusion process integrates multi-view embeddings by hierarchical autoencoders to obtain more versatile node embeddings.

d' is the unified dimension. σ means the activation function, such as ReLU [38].

The node feature transformation unifies the feature dimensions and facilitates the usage of subsequent modules. However, it should be noted that the heterogeneity has not been resolved. Although the dimensions of the feature vector of all nodes are the same, they still lie in different embedding spaces, so they should not be aggregated directly.

4.2 View-specific Ego Graph Encoding

Considering the **heterogeneity** and **semantics** of HGs, the local structure of the target node in HGs is rather complex. In this module, we treat each semantic P as the view to observe the target node's local structure. Therefore, the original complete ego graph can be decomposed into multiple view-specific ego graphs. The advantage of this operation is that multiple semantics can be decoupled. Another benefit is that the view-specific ego graph has better characteristics: there is only one type of nodes in the same order, and there is only one type of relation between different orders. Moreover, the view-specific ego graph only contains one kind of semantics.

Given a metapath $P = A_1 \xrightarrow{R_1} A_2 \xrightarrow{R_2} \dots \xrightarrow{R_{N-1}} A_N$ and a target node v with $\phi(v) = A_N$, the view-specific ego graph \mathcal{EG}_v^P preserves the complete local structure under semantic P with a multi-hop structure. The nodes of the i th hop have the same node type A_{N-i} and the relation between the i th hop and the $(i-1)$ th hop ($i \geq 1$) is R_{N-i} . In order to handle the heterogeneity and encode the structural and feature information sufficiently from the ego graph, we develop an ego graph encoder, which has two advantages. First, it can aggregate node features guided by the structure of the view-specific ego graph. Second, it models the representation of edges to handle the heterogeneity in the ego graph.

Two example of view-specific ego graph encoding is illustrated in Figure 2(b). Assuming that level 1 is the bottom level and level K is the top level, ego graph encoder aggregates information from level 1 to K , updating the representation $\mathbf{h}_i^{(l)} \in \mathbb{R}^{d'}$ of each node i at level l . The aggregation process (blue region in Figure 2(b)) between any intermediate two levels is illustrated

in Figure 3. Specifically, we set the hidden state of node i at level 1 as $\mathbf{h}_i^{(1)} = \mathbf{h}_i$, which is generated by the node feature transformation module. For any specific node i at level l ($l \neq 1$), we first aggregate its neighborhood information and then apply an activation function. Combined with its own features, the encoded feature is calculated as

$$\mathbf{h}_i^{(l)} = o(\mathbf{h}_i + \sigma(\text{Agg}(\{\mathbf{h}_j^{(l-1)}, v_j \in \mathcal{N}_i^{(l-1)}\}, \mathbf{h}_r^l))), \quad (2)$$

where $\mathbf{h}_i^{(l)} \in \mathbb{R}^{d'}$ is the encoded hidden vector of node i at level l , and $\mathbf{h}_i \in \mathbb{R}^{d'}$ is its initial state generated by the component of node content transformation. $\mathcal{N}_i^{(l-1)}$ is the neighborhood set of node i at level $(l-1)$, $\mathbf{h}_j^{(l-1)} \in \mathbb{R}^{d'}$ is the encoded hidden vector of node j at level $(l-1)$, \mathbf{h}_r^l is the representation of the relation r between level l and $(l-1)$. $\sigma(\cdot)$ is the ReLU activation function. Note that the representation is randomly initialized and optimized jointly with the network parameters. o is the dropout layer.

$\text{Agg}(\cdot)$ is an aggregate function to capture 1-hop neighborhoods information and relation representation:

$$\begin{aligned} & \text{Agg}(\{\mathbf{h}_j^{(l-1)}, v_j \in \mathcal{N}_i^{(l-1)}\}, \mathbf{h}_r^l) \\ &= \frac{1}{C_i} \sum_{v_j \in \mathcal{N}_i^{(l-1)}} \mathbf{W}_{\lambda(r)} \Phi(\mathbf{h}_j^{(l-1)}, \mathbf{h}_r^l), \end{aligned} \quad (3)$$

where $\Phi(\cdot, \cdot)$ is the mapping function for handling the heterogeneity, $\mathbf{W}_{\lambda(r)} \in \mathbb{R}^{d' \times d'}$ is the relation-specific message passing parameter, $C_i = |\mathcal{N}_i^{(l-1)}|$ is the normalization term.

For one thing, benefiting from the unified dimensions of all types of nodes, we can model the relations $\mathbf{h}_r^{(l)}$ as $\mathbb{R}^{d'}$ vectors and use the knowledge graph embedding approach to model the mapping function between the feature vectors of different types of nodes. Many functions can be adopted here and we apply TransE [36], which gains an impressive performance and efficiency in our experiments. In TransE [36], for a relation triplet (s, r, t) , there will be $\mathbf{s} + \mathbf{r} \approx \mathbf{t}$. Therefore:

$$\Phi(\mathbf{h}_s, \mathbf{h}_r) = \mathbf{h}_s + \mathbf{h}_r. \quad (4)$$

For another thing, the message passing parameter $\mathbf{W}_{\lambda(r)}$ would suffer from the over-parameterization problem with the

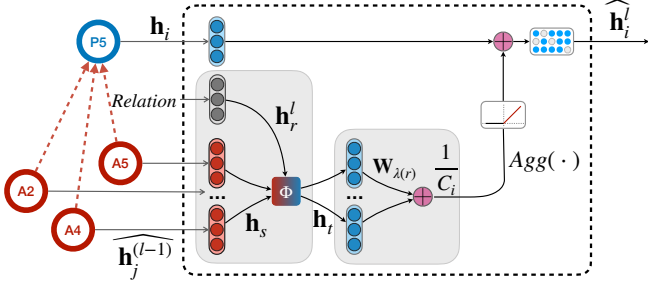


Fig. 3. Information aggregation for node P_5 at level l . The Author node's feature vector (\mathbf{h}_s), relation vector (\mathbf{h}_r^l), and P_5 's feature vector (\mathbf{h}_i) are aggregated to obtain new encoded feature vector for P_5 .

growth of the number of relations, since each relation r is associated with a matrix $\mathbf{W}_{\lambda(r)}$. Inspired by [14], [39], we simplify it to a direction-specific matrix, i.e., $\lambda(r) = \text{dir}(r)$, which is defined as follows:

$$\mathbf{W}_{\lambda(r)} = \mathbf{W}_{\text{dir}(r)} = \begin{cases} \mathbf{W}_O, & r \in \mathcal{R}^+ \\ \mathbf{W}_I, & r \in \mathcal{R}^- \end{cases}, \quad (5)$$

where \mathcal{R}^+ and \mathcal{R}^- are opposite sets of two relations. For example, $\mathcal{R}^+ = \{\text{write}, \text{publish}\}$ and $\mathcal{R}^- = \{\text{written by}, \text{published in}\}$. Note that the *self loop* relation can be randomly included in one of the two categories.

After $K - 1$ times of calculation on ego graph \mathcal{EG}_v^P , the representation of the target node v is $\mathbf{h}_v^{(K)}$. Note that the length of metapath is inconsistent. Note that the lengths of the metapaths are inconsistent, which results in different times of aggregation of Eq. (2).

$$\mathbf{h}_v^P = \frac{\mathbf{h}_v^{(K)}}{\text{depth}(\mathcal{EG}_v^P)} \quad (6)$$

where $\text{depth}(\mathcal{EG}_v^P)$ is the depth of the view-specific ego graph, which equals to the length of P .

In summary, given the features generated by the node feature transformation and the view set $\mathcal{P}_{A_i} = \{P_1, \dots, P_{|\mathcal{P}_{A_i}|}\}$ where the metapath start or end with the node type $A_i \in \mathcal{A}$, the view-specific ego graph encoding will generate a set of representations under each view for node $v \in \mathcal{A}_i$, denoted as $\{\mathbf{h}_v^{P_1}, \mathbf{h}_v^{P_2}, \dots, \mathbf{h}_v^{P_{|\mathcal{P}_{A_i}|}}\}$.

4.3 Auto Multi-view Fusion

After the view-specific ego graph encoding module, we get diverse representations of target nodes from each view. In this module, we will comprehensively fuse these representations to obtain better final representations with versatility. Versatility (as described in Definition 5) of multi-view representation learning is a crucial characteristic, which means the multi-view representation can perform at least as well as any single-view representations. In the following, we will show our proposed auto multi-view fusion and prove the result is superior to single view.

Given a metapath P_j in view set \mathcal{P}_{A_i} , we denote the embeddings of all nodes generated by view-specific ego graph encoding as $\mathbf{H}^{P_j} = [\mathbf{h}_1^{P_j}, \mathbf{h}_2^{P_j}, \dots, \mathbf{h}_{|\mathcal{V}_{A_i}|}^{P_j}]^T \in \mathbb{R}^{|\mathcal{V}_{A_i}| \times d}$. Therefore the representations from all views $\{\mathbf{H}^{P_1}, \mathbf{H}^{P_2}, \dots, \mathbf{H}^{P_{|\mathcal{P}_{A_i}|}}\}$ need be encoded into versatile representations \mathbf{H} . In order to do that, auto multi-view fusion utilizes hierarchical autoencoders

to preserve intra-view information and encode inter-view information simultaneously. We first demonstrate a standard autoencoder as $AE(\mathbf{X}; \Theta)$, where \mathbf{X} is the input of autoencoder and $\Theta = \{\mathbf{W}_{ae}^{(m)}, \mathbf{b}_{ae}^{(m)}\}_{m=1}^M$ is the network parameters with M being the number of layers. The first $\frac{M}{2}$ layers are the encoder network, and the last $\frac{M}{2}$ layers are the decoder network. Let $\mathbf{Z}^{(0)} = \mathbf{X}$, then the output of the m th layer is:

$$\mathbf{Z}^{(m)} = \sigma(\mathbf{Z}^{(m-1)} \mathbf{W}_{ae}^{(m)} + \mathbf{b}_{ae}^{(m)}), \quad (7)$$

where $\mathbf{Z}^{(m)} \in \mathbb{R}^{d_m}$. d_m is the output dimension of m -th layer. $\mathbf{W}_{ae}^{(m)} \in \mathbb{R}^{d_{m-1} \times d_m}$ and $\mathbf{b}_{ae}^{(m)} \in \mathbb{R}^{d_m}$ denote the weights and bias of the m th layer, respectively. $\sigma(\cdot)$ is the non-linear activation, such as ReLU [38]. For simplicity, we denote $f(\cdot; \Theta_e)$ as the encoder network where parameters $\Theta_e = \{\mathbf{W}_{ae}^{(m)}, \mathbf{b}_{ae}^{(m)}\}_{m=1}^{\frac{M}{2}}$ and $f(\cdot; \Theta_d)$ as the decoder network, where parameters $\Theta_d = \{\mathbf{W}_{ae}^{(m)}, \mathbf{b}_{ae}^{(m)}\}_{m=\frac{M}{2}+1}^M$. $f(\cdot)$ denotes general the multilayer perceptron architecture.

Firstly, in intra-view, we use view-specific autoencoders to compress the representations of each view to be more compact. Assuming the autoencoder under view P_j is $AE(\mathbf{H}^{P_j}; \Theta^{P_j})$, then the compressed representations, i.e., the output of the encoder network is:

$$\mathbf{Z}^{(\frac{M}{2}, P_j)} = f(\mathbf{H}^{P_j}; \Theta_e^{P_j}). \quad (8)$$

The reconstruction of the decoder network is:

$$\mathbf{Z}^{(M, P_j)} = f(\mathbf{Z}^{(\frac{M}{2}, P_j)}; \Theta_d^{P_j}). \quad (9)$$

Therefore, the reconstruction loss for all view-specific autoencoders is:

$$\mathcal{L}_{re}^{intra} = \frac{1}{2} \sum_{P_j} \|\mathbf{H}^{P_j} - \mathbf{Z}^{(M, P_j)}\|_F^2. \quad (10)$$

Secondly, in inter-view, we use a 2-layer supervised autoencoder [40] to encode all information into a latent representation comprehensively. We first concatenate the compressed representations from all views, denoted as $\mathbf{Z}^{\frac{M}{2}} = [\mathbf{Z}^{(\frac{M}{2}, P_1)}, \dots, \mathbf{Z}^{(\frac{M}{2}, P_{|\mathcal{P}_{A_i}|})}]$. Assuming the supervised autoencoder network is $AE(\mathbf{Z}^{\frac{M}{2}}; \Theta^s)$, where $\Theta^s = \{\mathbf{W}_s^1, \mathbf{W}_s^2, \mathbf{b}_s^1, \mathbf{b}_s^2\}$ and $\mathbf{W}_s^1 \in \mathbb{R}^{(d^{\frac{M}{2}} \cdot |\mathcal{P}_{A_i}|) \times d}$ and $\mathbf{W}_s^2 \in \mathbb{R}^{d \times (d^{\frac{M}{2}} \cdot |\mathcal{P}_{A_i}|)}$ and $\mathbf{b}_s^1 \in \mathbb{R}^d$ and $\mathbf{b}_s^2 \in \mathbb{R}^{d^{\frac{M}{2}} \cdot |\mathcal{P}_{A_i}|}$, then the output of the encoder network is:

$$\mathbf{H} = f(\mathbf{Z}^{\frac{M}{2}}; \Theta_e^s) = \sigma(\mathbf{Z}^{\frac{M}{2}} \mathbf{W}_s^1 + \mathbf{b}_s^1). \quad (11)$$

The reconstruction of the decoder network is:

$$\mathbf{Z}_{re}^{\frac{M}{2}} = f(\mathbf{H}; \Theta_d^s) = \sigma(\mathbf{H} \mathbf{W}_s^2 + \mathbf{b}_s^2). \quad (12)$$

Therefore, the reconstruction loss for the supervised autoencoders is:

$$\mathcal{L}_{re}^{inter} = \frac{1}{2} \|\mathbf{Z}_{re}^{\frac{M}{2}} - \mathbf{Z}^{\frac{M}{2}}\|_F^2. \quad (13)$$

The supervised information is the downstream task loss and will be discussed in Section 4.5.

Ideally, minimizing Eq. (10) and Eq. (13) will offer versatility to the multi-view representations $\mathbf{H} \in \mathbb{R}^{|\mathcal{V}_{A_i}| \times d}$, i.e., the final representations of all nodes of type A_i . Here we give a brief theoretical proof:

Proposition 1. (Versatility of the Multi-View Representation)

H) There exists a solution to Eq. (13) and Eq. (10) which holds the versatility.

Proof 1. First, we partition the weight parameter matrix of the decoder of the 2-layer supervised autoencoder as:

$$\mathbf{W}_s^2 = [(\mathbf{W}_s^2)^{P_1}, \dots, (\mathbf{W}_s^2)^{P_{|\mathcal{P}_{A_i}|}}], \quad (14)$$

where $(\mathbf{W}_s^2)^{P_j} \in \mathbb{R}^{|\mathcal{V}_{A_i}| \times d \frac{M}{2}}$. According to Eq. (13), it is easy to show that there exists $\mathbf{Z}^{(\frac{M}{2}, P_j)} = \sigma(\mathbf{H}(\mathbf{W}_s^2)^{P_j} + \mathbf{b}_s^2) = f(\mathbf{H}; \Theta_d^{(s, P_j)})$, where $f(\cdot; \Theta_d^{(s, P_j)})$ is the mapping from the multi-view representation \mathbf{H} to the compressed single view representation $\mathbf{Z}^{(\frac{M}{2}, P_j)}$. Further, according to Eq. (10), there exists $\mathbf{H}^{P_j} = f(\mathbf{Z}^{(\frac{M}{2}, P_j)}; \Theta_d^{P_j})$. Consequently, there exists:

$$\mathbf{H}^{P_j} = f(f(\mathbf{H}; \Theta_d^{(s, P_j)}); \Theta_d^{P_j}) = f(\mathbf{H}; \{\Theta_d^{(s, P_j)}, \Theta_d^{P_j}\}), \quad (15)$$

where $f(\cdot; \{\Theta_d^{(s, P_j)}, \Theta_d^{P_j}\})$ is the mapping from \mathbf{H} to \mathbf{H}^{P_j} . Hence, $\forall \varphi(\cdot)$ with $\mathbf{Y}^{P_j} = \varphi(\mathbf{H}^{P_j})$, there exists a mapping $\psi(\cdot)$ satisfying $\mathbf{Y}^{P_j} = \psi(\mathbf{H})$ by defining $\psi(\cdot) = \varphi(f(\cdot; \{\Theta_d^{(s, P_j)}, \Theta_d^{P_j}\}))$.

4.4 Regularization

There exist two issues when applying auto multi-view fusion. First, the autoencoders may suffer from the over-parameterization problem. Since the graph datasets are often semi-supervised where only a few labels can be accessed, the optimization of autoencoders might be overfitting. Second, the representations from different views contain much redundant information. For example, the *Co-author* view and *Co-conference* view may share many paper and author nodes. In order to address these issues, we introduce orthogonal regularization to the encoder network of each autoencoder. On the one hand, due to the orthogonality constraint, only informative weights are non-zero. On the other hand, the orthogonal column vectors can be regarded as orthogonal bases, ensuring each encoded dimension represents a unique meaning, *i.e.*, independent of the other dimensions. [41]

Specifically, considering all the first $\frac{M}{2}$ layers of all autoencoders *ae*, the orthogonal loss is:

$$\mathcal{L}_{ortho} = \sum_{ae} \sum_m^{\frac{M}{2}} \|(\mathbf{W}_{ae}^m)^T (\mathbf{W}_{ae}^m) \odot (\mathbf{I}_{d_m} - \mathbf{I}_{d_m})\|_1, \quad (16)$$

where \odot refers to the Hadamard product, *i.e.*, the element-wise product. We do not set orthogonal constraints on the decoder networks because the decoder needs to reconstruct the original hidden state that may contain many redundant features.

4.5 Optimization

In MV-HetGNN, we adopt a task-guided training strategy to optimize the network parameters. There are several strategies to optimize MV-HetGNN. For example, optimize view-specific ego graph encoding and auto multi-view fusion sequentially according to the downstream tasks. However, for the scalability and flexibility of the model, we optimize the MV-HetGNN in an **end-to-end** paradigm.

Specifically, according to the node labels' availability of downstream tasks, we divide them into two categories: semi-supervised and unsupervised downstream tasks. For semi-supervised learning (*e.g.*, node classification and node clustering), we first define the labeled node set as \mathcal{Y}_L and the downstream

classifier as $\mathbf{W}_C \in \mathbb{R}^{C \times d}$, where C is the number of classes. Then the downstream loss is:

$$\mathcal{L}_{ds} = - \sum_{v \in \mathcal{Y}_L} \mathbf{y}_v \ln(\mathbf{W}_C \mathbf{h}_v^T), \quad (17)$$

where the $\mathbf{h}_v \in \mathbb{R}^{1 \times d}$ and $\mathbf{y}_v \in \mathbb{R}^{1 \times C}$ is the embedding vector and one-hot label vector of labeled node v . For unsupervised learning (*e.g.*, link prediction), we design the loss function of preserving the graph structure, *i.e.*, the adjacency relationship of nodes. We optimize the model parameters by minimizing the following loss function through negative sampling [42]:

$$\mathcal{L}_{ds} = - \sum_{(u,v) \in \Omega} \log \sigma(\mathbf{h}_u^T \cdot \mathbf{h}_v) - \sum_{(u',v') \in \Omega^-} \log \sigma(-\mathbf{h}_{u'}^T \cdot \mathbf{h}_{v'}), \quad (18)$$

where $\sigma(\cdot)$ is the sigmoid function, Ω is the set of positive node pairs, and Ω^- is the sampled set of negative node pairs sampled from all unobserved node pairs.

Therefore, the complete loss function of MV-HetGNN is:

$$\mathcal{L} = \mathcal{L}_{ds} + \lambda(\mathcal{L}_{re}^{intra} + \mathcal{L}_{re}^{inter}) + \mathcal{L}_{ortho}, \quad (19)$$

where λ is a critical hyper-parameter that controls the degree of versatility. It is often a relatively small number, such as 0.1, 0.05. This is mainly because: i) At the beginning of training, the representation of each view is initialized almost randomly, so the reconstruction loss (*i.e.*, loss of generality) is meaningless. Therefore, in order to optimize the network parameter in the right direction, the downstream task loss needs to play a major role. ii) In practical cases, it is usually difficult to guarantee the exact versatility. Moreover, exactly versatile multi-view representation will loss flexibility for various datasets and downstream tasks.

We optimize the model parameters by minimizing \mathcal{L} via back-propagation and gradient descent. The overall learning algorithm is shown in Algorithm 1.

Algorithm 1: The overall learning algorithm of MV-HetGNN

Input: The graph $\mathcal{G} = (\mathcal{V}, \mathcal{E})$, the node features $\{\mathbf{H}_{A_i}, \forall A_i \in \mathcal{A}\}$, the view (metapath) set \mathcal{P} , the ego graphs $\mathcal{E}\mathcal{G}_v^P$ of each node v under each view P .

Output: The node Embeddings \mathbf{H} .

```

1 for node type  $A_i \in \mathcal{A}$  do
2   | Node feature transformation:  $\mathbf{H}'_{A_i} = \sigma(\mathbf{X}_{A_i} \mathbf{W}_{A_i})$ ;
3 end
4 for metapath  $P_j$  in  $\mathcal{P}$  do
5   | for node  $v \in \mathcal{V}$  do
6     | Given  $\mathcal{E}\mathcal{G}_v^{P_j}$ , calculate the view-specific
        representation  $\mathbf{h}_v^{P_j}$  by the view-specific ego
        graph encoding;
7   | end
8 end
9 Calculate multi-view representation  $\mathbf{H}$  by Eq. (8, 11);
10 Calculate the reconstruction loss by Eq. (10, 13);
11 Calculate the orthogonal regularization loss by Eq. (16);
12 Backpropagation and update parameters according to Eq.
    (19);
```

TABLE 2
Statistics of datasets.

Dataset	# Node	# Edge	Metapaths
DBLP	Author(A): 4,057 Paper(P): 2,081 Term(T): 7,723 Conference(C): 20	A-P: 19,645 P-T: 85,810 P-C: 14,328	APA APTPA APCPA
IMDb	Movie(M): 4,278 Director(D): 2,081 Actor(A): 5,257	M-D: 4,278 M-A: 12,828	MDM, MAM DMD, DMAMD AMA, AMDMA
Last.fm	User(U): 1,892 Artist(A): 17,632 Tag(T): 1,088	U-U: 12,717 U-A: 92,834 A-T: 23,253	UU, UAU UATAU, AUA AUUA, ATA

5 EXPERIMENTS

5.1 Experimental Setup

Dataset. As shown in Table 2, three heterogeneous graph datasets from different domains are used to evaluate the performance of MV-HetGNN. Following [9], [10], we use three widely used evaluation tasks: node classification, node clustering, and link prediction.

- **DBLP**¹: We adopt a subset of DBLP extracted by [43]. The authors are divided into four areas. DBLP is used for node classification and node clustering with data partition of 400 (9.86%), 400 (9.86%), and 3257 (80.28%) for training, validation, and testing.
- **IMDb**²: We adopt a subset of IMDb extracted by [10]. Each movie is labeled as one of three classes. IMDb is used for both node classification and node clustering with data partition of 400 (9.35%), 400 (9.35%), and 3478 (81.30%) nodes for training, validation, and testing, respectively.
- **Last.fm**³: We adopt a subset of Last.fm released by [44]. No label or features are included. Last.fm dataset is used for the link prediction task. All links are divided into training, validation, and testing set with data partition of 18567 (20%), 9283 (10%), and 64984 (70%), respectively.

Baselines. We compare MV-HetGNN with the following baselines:

- **Metapath2vec** [45] uses metapath-guided random walks and skip-gram model [46] to generate node embeddings. We test Metapath2vec++ [45] on all metapaths separately and report the best results.
- **HERec** [47] applies DeepWalk [48] on multiple metapath-based homogeneous graphs, and proposes an fusion algorithm for rating prediction. For node classification/clustering, we report the best result of all metapaths.
- **GCN** [6] performs convolutional operations in the graph Fourier domain.
- **GAT** [25] conducts convolutional operations in the spatial domain with the attention mechanism. We test GCN and GAT on metapath-based homogeneous graphs and report the best results.
- **HAN** [9] learns node embeddings from different metapath-based homogeneous graphs and leverages the attention mechanism to combine them into one vector for each node.

- **HGT** [16] designs node- and edge-type dependent parameters to characterize the heterogeneous attention over each edge to model heterogeneity.
- **MAGNN** [10] uses intra-metapath aggregation and inter-metapath aggregation to encode metapath instances, and learn the importance of different metapaths by an attention mechanism.

The above baselines can be divided into four categories. Metapath2vec and HERec are the traditional shallow heterogeneous graphs embedding models. GCN and GAT are conventional GNNs designed for homogeneous graphs. HGT is the first category of heterogeneous graph neural networks (as described in Section 2.2) HAN and MAGNN are the second category of heterogeneous graph neural networks.

Implementation. For Metapath2vec and HERec, we set the window size to 5, walk length to 100, walks per node to 40, and the number of negative samples to 5. For all GNNs, we set the dropout rate to 0.5 as default. For HAN, MAGNN, and HGT, we follow the original setting reported in these papers. For MV-HetGNN, we employ the Adam optimizer, and set the learning rate to 0.005, 0.001, 0.001 for DBLP and IMDb and Last.fm dataset, respectively. We set the number of layers of view-specific auto encoder M as 2. For the dimension hyper-parameters d' (output feature dimension of node feature transformation), $d^{\frac{M}{2}}$ (the output dimension of the encoder of view-specific autoencoder) and d (the dimension of multi-view representations), we set $d' = 2d^{\frac{M}{2}} = 2d$ for DBLP, and $d' = d^{\frac{M}{2}} = d$ for IMDb and $d' = d^{\frac{M}{2}} = d$ for Last.fm datasets, respectively.

5.2 Experimental Results

Node Classification. We conduct node classification experiments [9], [10] on the DBLP and IMDb datasets, with about 10% data used for training. After obtaining embeddings of labeled data by each model, we feed the testing nodes into a linear support vector machine (SVM) classifier with varying training proportions. Since the variance of graph-structured data can be relatively high, we repeat it ten times and report the averaged *Macro-F1* and *Micro-F1* in Table 3.

As shown in the table, the bold and underlined numbers indicate the best and runner-up results in the row, respectively. MV-HetGNN consistently achieves the best performance. The traditional shallow models (Metapath2vec and HERec) perform worse than GCN or GAT, since they do not leverage node content features. HAN obtains better performance than GAT and GCN because it exploits multiple metapaths to explore various semantics. HGT and MAGNN are able to outperform HAN because they can utilize more node features by stacking multilayer or metapath encoder, respectively. MV-HetGNN consistently outperforms HGT, which stacks multiple layers to catch high-order semantics. In contrast, MV-HetGNN employs the view-specific ego graph encoding to utilize higher-order information effectively. MV-HetGNN also obtains better results than MAGNN. There are two main reasons. For one thing, MV-HetGNN model the metapath-based local structure more comprehensively than MAGNN. For another thing, MV-HetGNN can comprehensively integrate the embeddings from different views to obtain more versatile node embeddings while MAGNN use attention only to softly *select* metapaths.

Node Clustering. We conduct node clustering experiments on the DBLP and IMDb datasets, using the same setting as [9],

1. <https://dblp.uni-trier.de/>

2. <https://www.imdb.com/>

3. <https://www.last.fm/>

TABLE 3
Results (%) on the DBLP and IMDB datasets for node classification task.

Dataset	Metrics	Train %	Unsupervised		Semi-supervised					
			Metapath2vec	HERec	GCN	GAT	HAN	HGT	MAGNN	MV-HetGNN
IMDb	Macro-F1	20%	45.94	45.31	53.63	54.74	57.52	59.38	59.48	61.33
		40%	47.41	46.63	53.86	56.27	57.81	59.91	59.79	61.43
		60%	48.23	47.07	54.22	56.97	58.28	60.32	60.02	61.39
		80%	50.34	48.02	54.77	57.43	58.69	60.38	60.20	61.89
	Micro-F1	20%	47.47	46.19	53.61	54.56	57.79	59.42	59.27	61.31
		40%	48.69	48.03	53.88	56.17	58.77	60.08	59.92	61.43
		60%	49.54	48.41	54.19	56.89	59.11	60.27	60.14	61.36
		80%	50.47	49.57	54.12	57.48	59.57	60.44	60.21	61.89
	Macro-F1	20%	89.39	90.31	90.00	91.37	91.87	92.05	93.01	95.23
		40%	89.99	91.15	90.11	91.70	92.36	92.57	93.24	95.31
		60%	90.31	92.01	90.12	91.76	92.80	92.90	93.52	95.34
		80%	90.94	92.37	91.07	93.81	93.01	93.40	93.79	95.44
DBLP	Macro-F1	20%	90.43	91.49	90.03	91.89	92.48	92.55	93.51	95.52
		40%	90.99	92.05	90.31	92.17	92.90	93.08	93.74	95.64
		60%	91.33	92.66	90.31	92.32	93.35	93.38	94.01	95.56
	Micro-F1	80%	91.61	92.78	90.40	92.36	93.53	93.46	94.17	95.80

TABLE 4
Results (%) on the DBLP and IMDB datasets for node clustering task.

Dataset	Metrics	Unsupervised		Semi-supervised					
		metapath2vec	HERec	GCN	GAT	HAN	HGT	MAGNN	MV-HetGNN
IMDb	NMI	0.93	0.41	8.10	9.98	12.46	14.50	14.41	16.37
	ARI	0.32	0.17	6.62	9.02	11.21	15.92	15.22	17.90
DBLP	NMI	74.09	69.31	72.75	75.03	77.86	77.47	80.52	84.73
	ARI	78.32	72.71	73.13	81.73	83.23	81.84	85.68	89.38

[10]. We feed the embeddings of labeled nodes to a K-Means algorithm. The number of cluster K is set to 3 for IMDb and 4 for DBLP. Since the clustering result of the K-Means algorithm is highly dependent on the initialization of the centroids, we repeat K-Means 10 times and report the averaged *normalized mutual information* (NMI) and *adjusted Rand index* (ARI).

The results are reported in Table 4. Overall, the relative performance of node clustering task is similar to the node classification task. MV-HetGNN significantly performs much better than all baselines consistently. The experimental results demonstrate that MV-HetGNN is able to learn more effective representation for the nodes of heterogeneous graphs. We note that the performance of all evaluated models on IMDb is much worse than on DBLP because every movie node has multiple genres in the original IMDb dataset, but only the first one is chosen as its class label.

Link Prediction. We evaluate the performance of link prediction task on Last.fm, following the MAGNN model [10]. Compared to MAGNN [10], we adopt a lower training ratio (only 20% links are used for training), which is a more challenging setting. The connected user-artist pairs are treated as positive links, while unconnected user-artist pairs are regarded as negative links.

We add the same number of randomly sampled negative node pairs to the validation and testing sets. The GNNs are then optimized by minimizing Equation 18. Given the user embedding \mathbf{h}_u and the artist embedding \mathbf{h}_a generated by the trained model, the linking probability of u and a is calculated by $Prob_{ua} = \sigma(\mathbf{h}_u^T \cdot \mathbf{h}_a)$, where σ is the commonly used sigmoid function. The embedding models are evaluated by the *area under the ROC curve* (AUC) and *average precision* (AP) scores. In Table 5, we report the averaged results of 10 runs of each embedding

model.

HAN outperforms Metapath2vec, GCN, and GAT, showing that considering multiple metapaths is crucial to generate more comprehensive node embeddings. Compared with HAN, both HGT and MAGNN are able to achieve large improvements. MV-HetGNN outperforms all baseline models by a large margin. Specifically, MV-HetGNN achieves a considerable improvement of around 6% over all baselines, indicating the superiority of MV-HetGNN. Compared with other methods, MV-HetGNN can effectively obtain high-order information, and comprehensively use the features and semantic information.

5.3 Ablation Study

We further conduct experiments on different variants of MV-HetGNN to investigate the three components of MV-HetGNN. To study the importance of model the mapping function between heterogeneous nodes, we consider MV-HetGNN_{non-transe}, which directly aggregate heterogeneous feature with $\Phi(\mathbf{h}_s, \mathbf{h}_r) = \mathbf{h}_s$. To study the importance of auto multi-view fusion, we construct two variants of MV-HetGNN, MV-HetGNN_{single} and MV-HetGNN_{attn}. MV-HetGNN_{single} removes the auto multi-view fusion module, and only uses single metapath to training. We report the best result of all metapaths. MV-HetGNN_{attn} replace the auto multi-view fusion module with attention mechanism applied in MAGNN. To study the superiority of view-specific ego graph encoding, we consider MV-HetGNN_{inst}, which replace the view-specific ego graph encoding with metapath instance encoding applied in MAGNN.

The results of ablation study are stated in Table 6, where the reported scores are the average of the scores under different training proportions in Table 3. We can observe that

TABLE 5
Results (%) on the Last.fm datasets for link prediction task.

Dataset	Metrics	metapath2vec	HERec	GCN	GAT	HAN	HGT	MAGNN	MV-HetGNN
Last.fm	AUC	74.32	73.98	76.59	80.03	81.00	86.53	87.68	92.80
	AP	74.11	72.53	75.51	81.44	82.03	88.77	<u>89.25</u>	94.03

TABLE 6
Results (%) on three datasets for ablation study.

Variants	IMDb				DBLP				Last.fm	
	Macro-F1	Micro-F1	NMI	ARI	Macro-F1	Micro-F1	NMI	ARI	AUC	AP
MV-HetGNN _{non-transe}	60.80	60.83	12.94	13.74	95.17	95.38	83.35	88.37	92.56	93.37
MV-HetGNN _{single}	58.15	57.41	10.62	11.74	94.47	94.86	80.74	83.72	87.43	90.79
MV-HetGNN _{attn}	60.14	60.19	12.77	13.32	94.12	94.51	79.16	83.31	92.69	94.31
MV-HetGNN _{inst}	60.48	60.47	15.39	16.08	94.37	94.66	81.36	86.71	88.76	89.74
MV-HetGNN	61.51	61.50	16.37	17.90	95.33	95.63	84.73	89.38	92.80	94.03

MV-HetGNN consistently achieves a performance improvement over MV-HetGNN_{non-transe}, which demonstrates the benefit of modelling the mapping function between heterogeneous nodes. The performance of MV-HetGNN_{single} is worse than the MV-HetGNN, which shows that it is necessary to consider multiple semantics. The performance of MV-HetGNN_{attn} is better than MV-HetGNN_{single} while worse than MV-HetGNN, which demonstrates that softly *select* strategy isn't enough for comprehensively integrate multi-view information, and the multi-view representation learning idea does help. The performance of MV-HetGNN_{inst} is worse than MV-HetGNN, which shows that the *sequence-level* encoding loses information when aggregating information from view-specific local structure.

5.4 Parameter Sensitivity

In this section, we conduct experiments to analyze the impacts of two critical hyper-parameters. In Figure 4, we present the results of NMI in node clustering and Macro-F1 in node classification on the IMDb dataset with different parameters.

First, we test sensitivity of the representation feature dimension d of \mathbf{H} . According to the setting in Section 5.1, we additionally set $d' = d^{\frac{M}{2}} = d$. Note that we only set it for the convenience of the parameter sensitivity test. The effect of dimension d of the final embedding \mathbf{H} is shown in Figure 4(a). As the embedding dimension increases, the performance will gradually rise to the highest point and then drop slowly. This is because the smaller dimension is not enough to encode the heterogeneous feature information and semantic information, while the larger dimensions may introduce redundancy, making the training of the model insufficient.

Second, we test the sensitivity of λ in Eq. (19). Figure 4(b) reports the effect of λ . As discussed in the Section 4.5, considering various data sets and downstream tasks, too strong versatility constraints (higher λ) can harm the model performance. A relatively small value will improve the performance of MV-HetGNN. For example, assuming that complementary metapaths that are meaningful to downstream tasks coexist with meaningless metapaths, it is beneficial to integrate all the information from the complementary metapaths, but it is harmful to forcibly contain information from the meaningless metapaths.

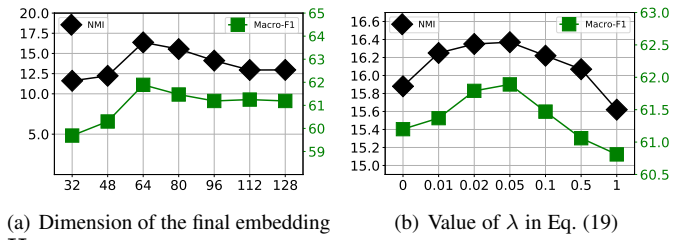


Fig. 4. Parameter sensitivity of MV-HetGNN

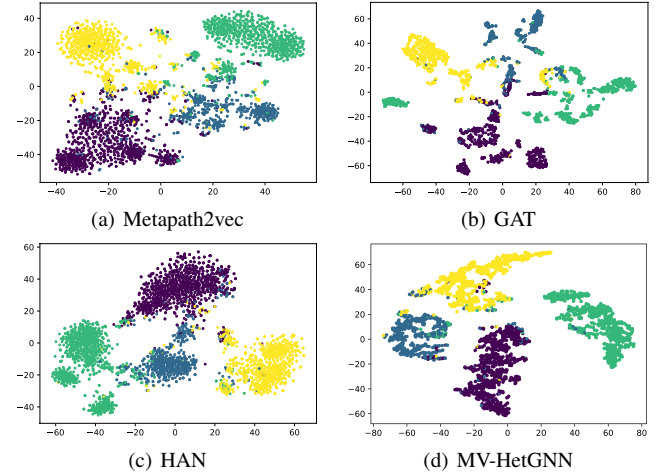


Fig. 5. Visualization of embeddings on DBLP. Each point denotes one author and its color indicates the research area.

5.5 Visualization

In this part, we conduct the task of visualization to intuitively compare the embedding results on a low dimensional space. First, we get the embeddings of the nodes in the testing set and then project them into a 2-dimensional space through t-SNE [49]. Due to the space limit, we only show the visualization of author embeddings in DBLP. As shown in Figure 5, GAT performs worst, where nodes of the same type are not closely distributed, and nodes with different types are mixed. Benefiting from the use of multiple metapaths to explore comprehensive semantic information, the visualization of HAN performs better than Metapath2vec and GAT. Further, MV-HetGNN achieves the best visualization performance. The nodes of the same type are located close to each

other, and the nodes from different types are well separated.

6 CONCLUSION

In this paper, we introduce the idea of multi-view representation learning to HGs embedding and propose a *Heterogeneous Graph Neural Networks with multi-view representation learning* (MV-HetGNN). Using the **semantics** property of HG, the complex ego graph in HGs is decomposed into multiple view-specific ego graphs. We conduct view-specific ego graph encoding to obtain node representation under each view. In this process, heterogeneity are addressed by learning the representation of relations to model the mapping relation between heterogeneous nodes. Then the auto multi-view fusion module is developed to integrate the embeddings from different views. More versatile node embeddings with theoretically guarantee are learned in this module. We conduct extensive experiments on three real-world datasets, and the results show that the proposed MV-HetGNN significantly outperforms all the state-of-the-art baselines on various tasks.

REFERENCES

- [1] W. Fan, Y. Ma, Q. Li, Y. He, E. Zhao, J. Tang, and D. Yin, “Graph neural networks for social recommendation,” in *WWW*, 2019.
- [2] M. Zhang and Y. Chen, “Link prediction based on graph neural networks,” in *NeurIPS*, 2018.
- [3] R. Ying, R. He, K. Chen, P. Eksombatchai, W. L. Hamilton, and J. Leskovec, “Graph convolutional neural networks for web-scale recommender systems,” in *SIGKDD*, 2018.
- [4] M. Wang, Y. Lin, G. Lin, K. Yang, and X.-m. Wu, “M2grl: A multi-task multi-view graph representation learning framework for web-scale recommender systems,” in *SIGKDD*, 2020.
- [5] W. Hamilton, Z. Ying, and J. Leskovec, “Inductive representation learning on large graphs,” in *NeurIPS*, 2017.
- [6] T. N. Kipf and M. Welling, “Semi-supervised classification with graph convolutional networks,” in *ICLR*, 2017.
- [7] J. You, J. M. Gomes-Selman, R. Ying, and J. Leskovec, “Identity-aware graph neural networks,” in *Proceedings of the AAAI Conference on Artificial Intelligence*, vol. 35, no. 12, 2021, pp. 10 737–10 745.
- [8] X. Wang, D. Bo, C. Shi, S. Fan, Y. Ye, and P. S. Yu, “A survey on heterogeneous graph embedding: Methods, techniques, applications and sources,” *arXiv preprint arXiv:2011.14867*, 2020.
- [9] X. Wang, H. Ji, C. Shi, B. Wang, Y. Ye, P. Cui, and P. S. Yu, “Heterogeneous graph attention network,” in *WWW*, 2019.
- [10] X. Fu, J. Zhang, Z. Meng, and I. King, “Magnn: Metapath aggregated graph neural network for heterogeneous graph embedding,” in *WWW*, 2020.
- [11] M. Schlichtkrull, T. N. Kipf, P. Bloem, R. Van Den Berg, I. Titov, and M. Welling, “Modeling relational data with graph convolutional networks,” in *ESWC*, 2018.
- [12] H. Hong, H. Guo, Y. Lin, X. Yang, Z. Li, and J. Ye, “An attention-based graph neural network for heterogeneous structural learning,” in *AAAI*, 2020.
- [13] C. Zhang, D. Song, C. Huang, A. Swami, and N. V. Chawla, “Heterogeneous graph neural network,” in *SIGKDD*, 2019.
- [14] S. Vashishth, S. Sanyal, V. Nitin, and P. P. Talukdar, “Composition-based multi-relational graph convolutional networks,” in *ICLR*, 2020.
- [15] X. Qin, N. Sheikh, B. Reinwald, and L. Wu, “Relation-aware graph attention model with adaptive self-adversarial training,” in *Proceedings of the AAAI Conference on Artificial Intelligence*, vol. 35, no. 11, 2021, pp. 9368–9376.
- [16] Z. Hu, Y. Dong, K. Wang, and Y. Sun, “Heterogeneous graph transformer,” in *WWW*, 2020.
- [17] S. Fan, J. Zhu, X. Han, C. Shi, L. Hu, B. Ma, and Y. Li, “Metapath-guided heterogeneous graph neural network for intent recommendation,” in *Proceedings of the 25th ACM SIGKDD International Conference on Knowledge Discovery & Data Mining*, 2019, pp. 2478–2486.
- [18] F. Xu, J. Lian, Z. Han, Y. Li, Y. Xu, and X. Xie, “Relation-aware graph convolutional networks for agent-initiated social e-commerce recommendation,” in *Proceedings of the 28th ACM international conference on information and knowledge management*, 2019, pp. 529–538.
- [19] Z. Qiao, P. Wang, Y. Fu, Y. Du, P. Wang, and Y. Zhou, “Tree structure-aware graph representation learning via integrated hierarchical aggregation and relational metric learning,” *arXiv preprint arXiv:2008.10003*, 2020.
- [20] H. Ji, J. Zhu, X. Wang, C. Shi, B. Wang, X. Tan, Y. Li, and S. He, “Who you would like to share with? a study of share recommendation in social e-commerce,” in *Proceedings of the AAAI Conference on Artificial Intelligence*, vol. 35, no. 1, 2021, pp. 232–239.
- [21] C. Zhang, Y. Cui, Z. Han, J. T. Zhou, H. Fu, and Q. Hu, “Deep partial multi-view learning,” *IEEE transactions on pattern analysis and machine intelligence*, 2020.
- [22] C. Zhang, Y. Liu, and H. Fu, “Ae2-nets: Autoencoder in autoencoder networks,” in *Proceedings of the IEEE/CVF Conference on Computer Vision and Pattern Recognition*, 2019, pp. 2577–2585.
- [23] J. Bruna, W. Zaremba, A. Szlam, and Y. LeCun, “Spectral networks and locally connected networks on graphs,” in *ICLR*, 2014.
- [24] M. Defferrard, X. Bresson, and P. Vandergheynst, “Convolutional neural networks on graphs with fast localized spectral filtering,” in *NeurIPS*, 2016.
- [25] P. Velickovic, G. Cucurull, A. Casanova, A. Romero, P. Liò, and Y. Bengio, “Graph attention networks,” in *ICLR*, 2018.
- [26] J. Gilmer, S. S. Schoenholz, P. F. Riley, O. Vinyals, and G. E. Dahl, “Neural message passing for quantum chemistry,” in *ICML*, 2017.
- [27] A. Vaswani, N. Shazeer, N. Parmar, J. Uszkoreit, L. Jones, A. N. Gomez, Ł. Kaiser, and I. Polosukhin, “Attention is all you need,” in *NeurIPS*, 2017.
- [28] X. Wang, M. Zhu, D. Bo, P. Cui, C. Shi, and J. Pei, “Am-gcn: Adaptive multi-channel graph convolutional networks,” in *SIGKDD*, 2020.
- [29] P. Li, Y. Wang, H. Wang, and J. Leskovec, “Distance encoding: Design provably more powerful neural networks for graph representation learning,” *NeurIPS*, 2020.
- [30] K. Xu, W. Hu, J. Leskovec, and S. Jegelka, “How powerful are graph neural networks?” in *ICLR*, 2019.
- [31] Y. Cen, X. Zou, J. Zhang, H. Yang, J. Zhou, and J. Tang, “Representation learning for attributed multiplex heterogeneous network,” in *SIGKDD*, 2019.
- [32] C. Zhang, A. Swami, and N. V. Chawla, “Shne: Representation learning for semantic-associated heterogeneous networks,” in *WSDM*, 2019.
- [33] Y. Fu, Y. Xiong, S. Y. Philip, T. Tao, and Y. Zhu, “Metapath enhanced graph attention encoder for hins representation learning,” in *2019 IEEE International Conference on Big Data (Big Data)*, 2019.
- [34] S. Yun, M. Jeong, R. Kim, J. Kang, and H. J. Kim, “Graph transformer networks,” in *NeurIPS*, 2019.
- [35] S. Zhu, C. Zhou, S. Pan, X. Zhu, and B. Wang, “Relation structure-aware heterogeneous graph neural network,” in *ICDM*, 2019.
- [36] A. Bordes, N. Usunier, A. Garcia-Duran, J. Weston, and O. Yakhnenko, “Translating embeddings for modeling multi-relational data,” *NeurIPS*, 2013.
- [37] B. Yang, W.-t. Yih, X. He, J. Gao, and L. Deng, “Embedding entities and relations for learning and inference in knowledge bases,” *arXiv preprint arXiv:1412.6575*, 2014.
- [38] V. Nair and G. E. Hinton, “Rectified linear units improve restricted boltzmann machines,” in *ICML*, 2010.
- [39] D. Marcheggiani and I. Titov, “Encoding sentences with graph convolutional networks for semantic role labeling,” in *EMNLP*, 2017.
- [40] L. Le, A. Patterson, and M. White, “Supervised autoencoders: Improving generalization performance with unsupervised regularizers,” *Advances in neural information processing systems*, vol. 31, pp. 107–117, 2018.
- [41] C. Ranjan, *Understanding Deep Learning Application in Rare Event Prediction*. Connaissance Publishing, 2020.
- [42] T. Mikolov, I. Sutskever, K. Chen, G. S. Corrado, and J. Dean, “Distributed representations of words and phrases and their compositionality,” *NeurIPS*, 2013.
- [43] M. Ji, Y. Sun, M. Danilevsky, J. Han, and J. Gao, “Graph regularized transductive classification on heterogeneous information networks,” in *ECML PKDD*, 2010.
- [44] I. Cantador, P. Brusilovsky, and T. Kuflik, “2nd workshop on information heterogeneity and fusion in recommender systems (hetrec 2011),” in *RecSys*, 2011.
- [45] Y. Dong, N. V. Chawla, and A. Swami, “metapath2vec: Scalable representation learning for heterogeneous networks,” in *SIGKDD*, 2017.
- [46] T. Mikolov, K. Chen, G. Corrado, and J. Dean, “Efficient estimation of word representations in vector space,” in *ICLR*, 2013.
- [47] C. Shi, B. Hu, W. X. Zhao, and S. Y. Philip, “Heterogeneous information network embedding for recommendation,” *TKDE*, 2018.
- [48] B. Perozzi, R. Al-Rfou, and S. Skiena, “Deepwalk: Online learning of social representations,” in *SIGKDD*, 2014.

[49] L. Van der Maaten and G. Hinton, “Visualizing data using t-sne.” *JMLR*, 2008.

ACKNOWLEDGMENTS

The research work is partially supported by the National Natural Science Foundation of China under Grant No. 61902376.



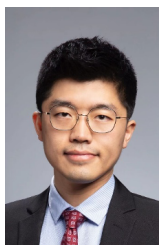
Shao zezhi received the B.E. degree from Shandong University, Jinan, China, in 2019. He is currently pursuing a Ph.D. degree with the Institute of Computing Technology, Chinese Academy of Sciences, China. His research interests include graph and data mining.



Yongjun Xu is a professor at Institute of Computing Technology, Chinese Academy of Sciences (ICT-CAS) in Beijing, China. He received his B.Eng. and Ph.D. degree in computer communication from Xi'an Institute of Posts & Telecoms (China) in 2001 and Institute of Computing Technology, Chinese Academy of Sciences, Beijing, China in 2006, respectively. His current research interests include artificial intelligence systems, and big data processing.



Wei Wei received the Ph.D. degree from the Huazhong University of Science and Technology, Wuhan, China, in 2012. He is currently an Associate Professor with the School of Computer of Science and Technology, Huazhong University of Science and Technology. His current research interests include information retrieval, natural language processing, text mining, artificial intelligence, machine learning, and social computing.



Fei Wang, born in 1988, PhD, associate professor. He received the B.S. degree in computer science from the Beijing Institute of Technology, Beijing, China, in 2011. He received the PhD degree in computer architecture from Institute of Computing Technology, Chinese Academy of Sciences in 2017. From 2017 to 2020, he was a research assistant with the Institute of Technology, Chinese Academy of Sciences. Since 2020, he has been working as associate professor in Institute of Computing Technology, Chinese Academy of Sciences. His main research interest includes spatiotemporal data mining, Information fusion, graph neural networks.



Zhao Zhang is a research associate at the Institute of Computing Technology, Chinese Academy of Sciences, Beijing, China. He received the B.E. degree in Computer Science and Technology from the Beijing Institute of Technology (BIT) in 2015, and Ph.D. degree in the Institute of Computing Technology, Chinese Academy of Sciences in 2021. His current research interests include data mining and knowledge graphs.



bioinformatics.

Feida Zhu received the B.S. degree in computer science from Fudan University, Shanghai, China, and the Ph.D. degree in computer science from the University of Illinois at Urbana-Champaign, Champaign, IL, USA. He is an Assistant Professor with the School of Information Systems, Singapore Management University, Singapore. His current research interests include large-scale graph pattern mining and social network analysis, with applications on Web, management information systems, business intelligence, and